Modeling of Critical Heat Flux in Light-Water Flow with Heavy-Water-Based Correlation[1]

L.K.H. Leung
Advanced Concepts and Collaboration, Chalk River Laboratories
Atomic Energy of Canada Limited, Chalk River, Ontario, Canada K0J 1J0

Abstract

Critical heat flux (CHF) data were obtained with light-water flow over a 37-element bundle simulator and were transformed into heavy-water-equivalent values using the fluid-to-fluid CHF modeling parameters. These equivalent values were used to derive a heavy-water-based CHF correlation for use in regional-overpower protection and safety analyses. The heavy-water-based CHF correlation has been assessed against the light-water CHF data for the 37-element bundle directly without applying the fluid-to-fluid modeling parameters. The assessment indicated an underprediction of about 5% of the light-water CHF data. This implies that applying the light-water correlation would overpredict the heavy-water CHF data by a similar bias.

1. Introduction

Prediction of critical heat flux (CHF) in fuel bundles is essential for establishing the safety margin of pressurized heavy-water reactors. The majority of CHF data for fuel bundles were obtained with light-water experiments, due to the cost of heavy water. These data were transformed into heavy-water equivalent values, which have been applied in developing relevant correlations. In principle, these correlations must be implemented into reactor safety codes for safety analyses. Due to the proprietary nature of some safety codes, implementation of user-derived correlations is not feasible. In those cases, the light-water correlations implemented in the codes are applied in heavy-water analyses, based on the assumption that CHF behaviors are similar between light water and heavy water for the small differences in fluid properties.

The objective of this study is to quantify the potential impact of applying a light-water-based CHF correlation to heavy-water CHF analyses. Due to a lack of heavy-water CHF data for 37-element bundles (some data are available but are proprietary), a reversed assessment is performed to examine the impact of applying a heavy-water-based CHF correlation to light-water CHF data.

2. Fluid-to-Fluid Modelling of CHF

Transformation of CHF value and corresponding flow conditions from a modelling fluid to the working fluid is based on fluid-to-fluid modelling parameters. Becker [1] obtained heavy-water CHF data with a vertical tube of 10-mm inside diameter. He showed good agreement of these data with predictions of light-water CHF correlation when presenting the critical quality in terms of a dimensional CHF parameter.

A number of non-dimensional groups have been proposed as fluid-to-fluid modelling parameters for CHF [2], [3], [4]. Among them, those suggested by Ahmad [3] and Katto and Ohno [4] are the most

[1] AECL internal document identification "CW-125200-CONF-016 (Unrestricted)"

phenomeno-logically correct and have been recommended by Groeneveld et al. [5] and Tain [6]. The density ratio is used to model the system pressure between the two systems, i.e.,

$$\left(\frac{\rho_f}{\rho_g}\right)_{working} = \left(\frac{\rho_f}{\rho_g}\right)_{\text{modelling}} \tag{1}$$

The thermodynamic quality is used for the local enthalpy, i.e.,

$$x_{working} = x_{\text{modelling}} \tag{2}$$

The Weber number is used to model the mass flux [4], i.e.,

$$\left(\frac{GD^{1/2}}{\sigma^{1/2}\rho_f^{1/2}}\right)_{working} = \left(\frac{GD^{1/2}}{\sigma^{1/2}\rho_f^{1/2}}\right)_{\text{modelling}} \tag{3}$$

The boiling number is used for the CHF, i.e.,

$$\left(\frac{CHF}{GH_{fg}}\right)_{working} = \left(\frac{CHF}{GH_{fg}}\right)_{\text{modelling}} \tag{4}$$

Leung and Groeneveld [7] showed the applicability of these modelling parameters for transforming Freon CHF data to water-equivalent CHF values of the 37-element bundle. Figure 1 compares water CHF values for the horizontal 37-element bundle test against water-equivalent CHF values of the Freon data for the vertical 37-element bundle tests at the water-equivalent pressure of 10 MPa and mass flow rate of 17 $kg \cdot s^{-1}$. Three sets of Freon-12 data were obtained at different experimental stages; the slight differences exhibited in Set 2 have been attributed to measurement uncertainty. Leung and Groeneveld [7] showed similar Freon CHF values between horizontal and vertical 37-element bundles at high flows (or negligible orientation effect).

3. Full-Scale 37-Element Bundle Experiments in Light Water

Many experiments were performed with 37-element bundle simulators that were electrically heated with direct current and cooled with high-pressure light water inside horizontal channels [8]. The channel consisted of a steel shroud (pressure boundary) with an alumina liner insulating the heated bundle from the steel shroud. Loop conditions at both inlet and outlet ends of the channel were monitored with differential-pressure cells and either Chromel-Alumel (K-type) thermocouples or resistor temperature devices. In addition, pressure taps were installed at various locations along the bundle string to obtain pressure-drop data. Figure 2 illustrates the test station setup and instrumentation for experiments using the bundle-string simulator of non-uniform axial power profile at Stern Laboratories.

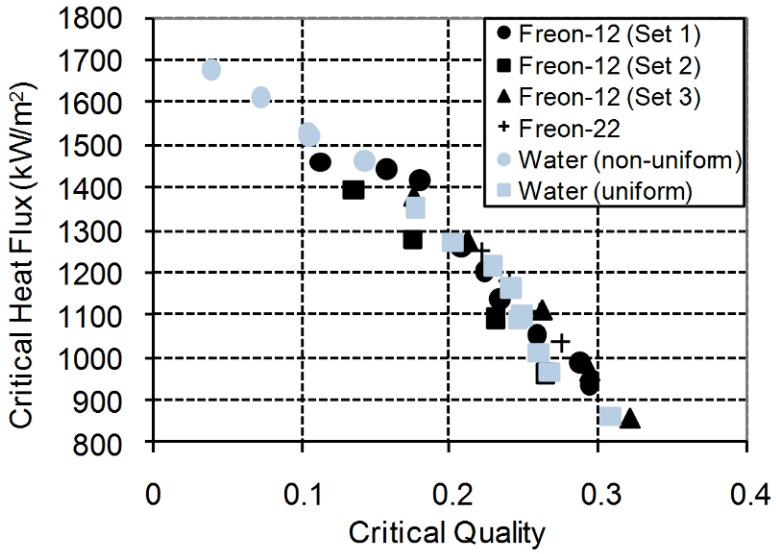

Figure 1 Comparison of CHF Values of Vertical Uniformly Heated Bundle Strings [7].

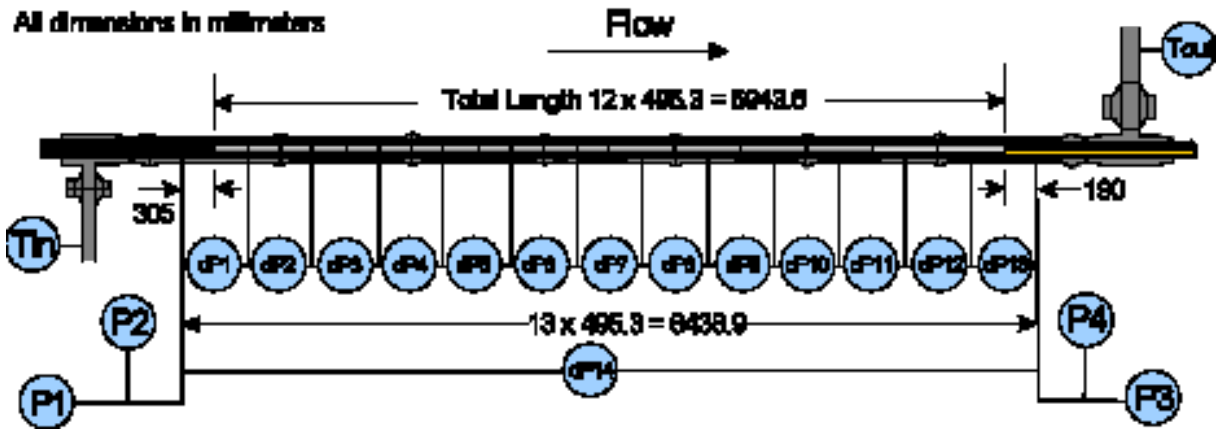

Figure 2 Locations of Loop Instrumentation in One of the Test Stations

The 37-element bundle simulator simulated twelve aligned 49.53-cm-long bundles. It consisted of elements having the same outer diameter as elements in a production bundle and was equipped with spacers and bearing pads at the designated locations over the entire length. The configuration of end plates, midplane spacers and bearing pads in the simulator resembled the Bruce 37-element fuel design (see Figure 3). Hollow spacers and bearing pads were used reducing the distortion of electric current. Initial dryout locations were detected using moveable thermo-couples installed inside elements of all rings.

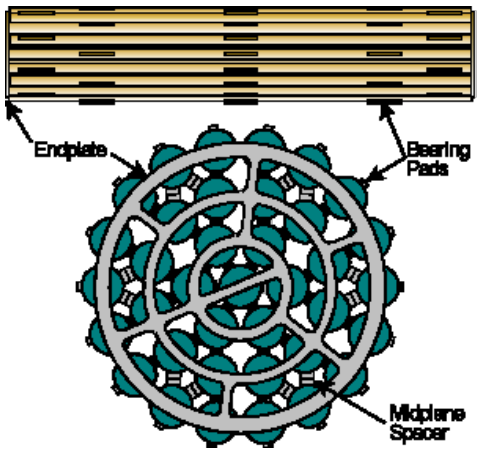

Figure 3 Bruce 37-Element Fuel Design

The moveable thermocouples were installed in a carrier, which was traversed axially and circumferentially inside the element, mapping the surface temperature distribution and detecting the first occurrence of CHF at any location. The sliding thermocouples assembly and a typical carrier is illustrated in Figure 4 with two sets of thermocouples. The dryout detection technique has evolved over the years; this has led to a more precise determination of dryout locations and CHF.

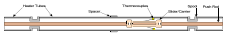

Figure 4 Sliding Thermocouples Assembly and Carrier

The bundle simulator exhibited a non-uniform radial power profile corresponding to that of the natural uranium fuel at mid-life burnup under low coolant density conditions (or end-of-life burnup under high coolant density conditions). The non-uniform radial power profile was implemented by varying the element thickness in various rings. Ratios of local element to cross-sectional average heat fluxes were 0.826, 0.859, 0.932 and 1.102 for the centre element, and elements in the inner ring, intermediate ring, and outer ring, respectively.

Two different axial power profiles were tested: uniform and downstream-skewed cosine profiles. The junction and appendage configurations are the same in bundle simulators of uniform and non-uniform axial power profile, and hence exhibit the same enhancement effect on dryout power for both simulators.

Experiments with a 37-element bundle having a uniform axial power profile were performed in the U-1 out-reactor loop at the Chalk River Laboratories [9]. Two experiments were performed using the bundle simulator having a uniform axial power profile. The first test utilized the full length of 12 bundles. In the second test, nickel tubes were introduced to replace Inconel tubes at the upstream half (i.e., six bundle segments) of the full-length bundle simulator reducing the overall heated length. Table 1 lists geometric dimensions of the simulators.

Table 1 Dimensions of Simulated Bruce-Bundle Strings with Uniform Axial Power Profile

Bundle	6-m	3-m
Element diameter (mm)	13.08	13.08
Element length (mm)	481.4	481.4
Overall bundle length (mm)	5943.6	5943.6
Element heated length (mm)	480.17	480.17
Overall heated length (mm)	5762.4	2881.2
Alumina liner I.D. (mm)	103.86	103.86
Overall heated area (m^2)	8.7612	4.3806
Flow area (mm^2)	3500	3500
Hydraulic diameter (mm)	7.58	7.58

The uniform-bundle experiments covered ranges of outlet pressures from 6.57 to 11.08 MPa, mass flow rates from 4.37 to 16.68 $kg \cdot s^{-1}$, and inlet fluid temperatures from 156 to 307°C.

Experiments with 37-element bundles having a non-uniform axial power profile were performed at both Chalk River Laboratories and Stern Laboratories. The non-uniform power profile was established using tapered tubes of various wall thickness values. Figure 5 illustrates the axial power profile for the non-uniform bundle simulators. The narrow strip between bundles corresponds to a 15-mm unheated length at each junction simulation. Simultaneous dryout occurrences were observed at several locations along the bundle string at some flow conditions. Table 2 lists geometric dimensions of the simulator. These experiments covered ranges of outlet pressures from 5.95 to 11.06 MPa, mass flow rates from 7.06 to 22.0 $kg \cdot s^{-1}$, and inlet fluid temperatures from 199 to 281°C.

Table 2 Dimensions of Simulated Bruce-Bundle String with Non-Uniform Axial Power Profile

Element diameter (mm)	13.06
Element length (mm)	481.4
Overall bundle length (mm)	5943.6
Element heated length (mm)	480.12
Overall heated length (mm)	5761.44
Alumina liner I.D. (mm)	103.86
Overall heated area (m^2)	8.744
Flow area (mm^2)	3519
Hydraulic diameter (mm)	7.63

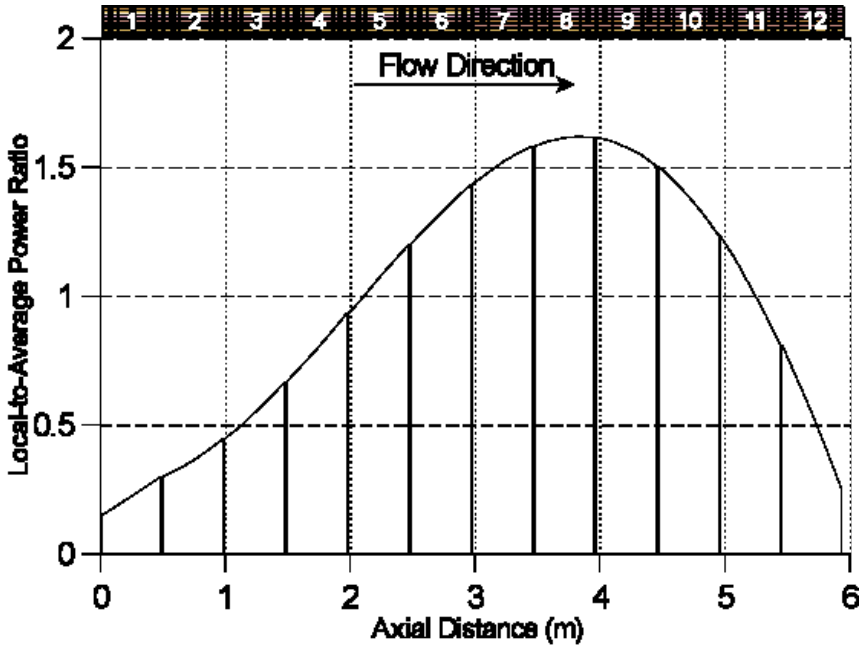

Figure 5 Non-Uniform Axial Power Profile

The experiments focused on the detection of the onset of intermittent dryout (OID) (i.e., the first sign of a rapid temperature rise detected by the thermocouples with a slight increase in power anywhere in the bundle string). The test-section power corresponding to the initial CHF occurrence was referred to as the dryout power. Dryout power measurements were obtained mainly at conditions of interest to normal operations, and postulated accidents such as loss of flow, small loss of coolant, and loss of regulation events.

4. Dryout Power Measurements and Critical Heat Flux

Figure 6 illustrates dryout power measurements for bundles with uniform and non-uniform axial power profiles obtained at pressures of 9 and 9.6 MPa, inlet fluid temperatures of 250 and 253°C for mass flow rate varying from 5 to 22 $kg \cdot s^{-1}$. Dryout powers are higher for the uniform axial power profile than the non-uniform axial power profile at high mass flow rates, but the difference diminishes with decreasing flow rate. Similar trends have been observed at other flow conditions.

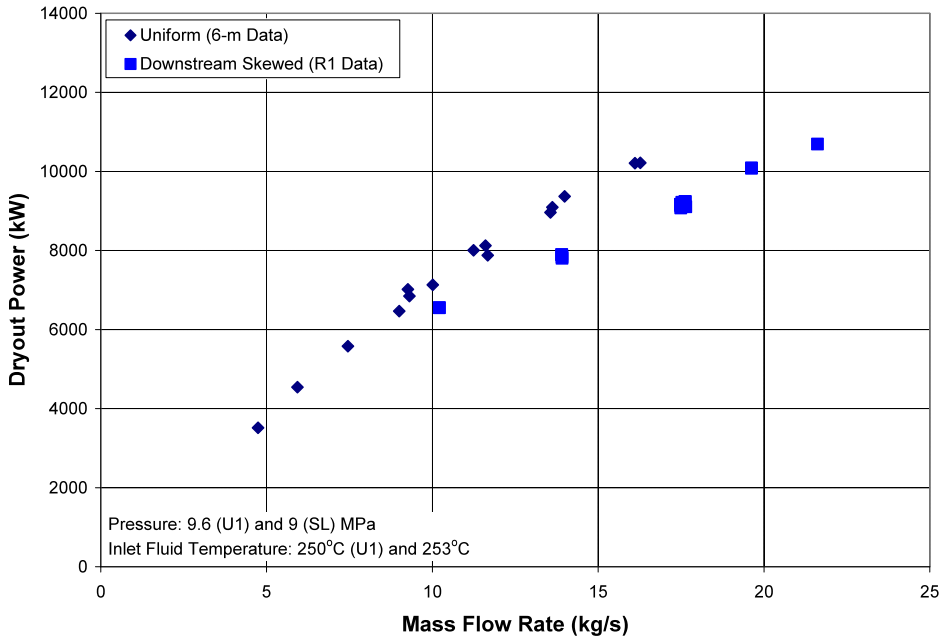

Figure 6 Dryout Power Measurements for Bundles of Uniform and Non-Uniform Axial Power Profiles

CHF values and dryout conditions have been established from the dryout power and dryout locations. Dryout was observed at the last (i.e., 12th) bundle of the string with a uniform axial power profile, where the fluid enthalpy is the highest. It was observed at locations just upstream of either the spacer or junction plane at the 10th or 11th bundles from the inlet (see Figure 5 for the identification of the bundle segment). The effect of axial power profile on CHF is accounted for using the boiling-length-average (BLA) heat flux approach for the CANDU 37-element bundle [8]. The BLA heat flux is defined as

$$q_{BLA} = \frac{1}{z_{DO} - z_{BI}} \int_{z_{BI}}^{z_{DO}} q_{local} dz \qquad (5)$$

where z_{DO} is the axial location at dryout in metres, z_{BI} is the axial location at boiling initiation in metres, and q_{local} is the local heat flux at various locations. The onset of significant void is adopted as the onset of bulk-boiling point taking into the account of enthalpy imbalance in the bundle. It has been established from the pressure profile along the channel and represented using a correlation.

Figure 7 compares BLA CHF values for 37-element bundles of uniform and non-uniform axial power profiles. The BLA CHF is the same as the local CHF for the bundle with uniform axial power profile.

Local CHF values for the bundle with the non-uniform axial power profile are also shown for comparison. Good agreement has been observed among CHF values between uniform and non-uniform profiles using the BLA heat flux approach.

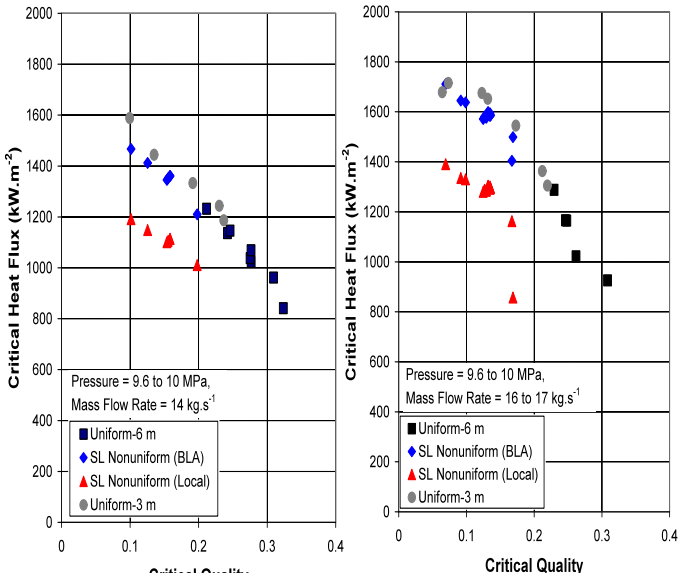

Figure 7 Comparison of CHF Values for 37-Element Bundles of Uniform and Non-Uniform Axial Power Profiles

5. Heavy-Water CHF Correlation for the CANDU 37-Element Bundle

The CHF values and corresponding flow conditions obtained with the 37-element bundle simulators of uniform and non-uniform axial power profiles from several selected light-water experiments were transformed into heavy-water-equivalent values. As illustrated in Figure 7, the CHF variation is non-linear over the full range of critical quality, but can be considered linear over the narrow ranges at low and high qualities. For simplicity, two separate correlations are derived to represent CHF values (in $MW \cdot m^{-2}$) in the low and high quality ranges and the minimum value calculated with these correlations are selected, i.e.,

$$q_{CHF} = Min\left(q_{CHF,\,low-quality}, q_{CHF,\,high-quality}\right)$$

$$q_{CHF,\,low-quality} = 2297.4\, P_{DO}^{-0.589}\, G_{DO}^{0.664} - 2226.2\, P_{DO}^{-1.122}\, G_{DO}^{1.531}\, x_{cr} \qquad (6)$$

$$q_{CHF,\,high-quality} = 2325.4\, P_{DO}^{-0.715}\, G_{DO}^{0.985} - 2051.1\, P_{DO}^{-0.852}\, G_{DO}^{1.706}\, x_{cr}$$

where P is the local pressure in MPa, G is the local mass flux in $Mg \cdot m^{-2} \cdot s^{-1}$, and x_{cr} is the critical quality. The correlation represents 284 data points of uniform and non-uniform axial power profiles for the 37-element bundle with an average error of 0.5% and a standard deviation of 6.7%. The average error is defined as

$$Average\,Error = \overline{Error} = \frac{1}{N}\sum_{i=1}^{N}(Error)_i \qquad (7)$$

and the standard deviation is defined as

$$Standard\ Deviation = \sigma_{error} = \sqrt{\frac{1}{N-1}\sum_{i=1}^{N}\left(Error - \overline{Error}\right)^2} \tag{8}$$

where N is the number of data points, and the prediction error is defined as

$$Error = \frac{Predicted\ CHF}{Experimental\ CHF} - 1 \tag{9}$$

6. Prediction of Light-Water Dryout Power using the Heavy-Water-Based Correlation

As indicated previously, most reactor safety codes have been developed for light-water applications and implementation of heavy-water correlations is rather cumbersome. Heavy-water properties, on the other hand, can be implemented through the input deck. Due to a lack of heavy-water dryout power measurements for the 37-element bundle, an assessment of the prediction accuracy for heavy-water dryout power measurements using the light-water-based correlation is not feasible. Therefore, the current study focuses on the assessment of the prediction accuracy for light-water dryout power measurements using the heavy-water-based correlation, derived in Section 5.

The heavy-water-based CHF correlation is assessed against light-water dryout power measurements for 37-element bundles of uniform and non-uniform axial power profiles. As indicated previously, the BLA heat-flux approach is applied to account for the effect of axial heat-flux distribution on CHF when assessing the measurements for the bundle with a non-uniform axial power profile. A systematic underprediction of dryout power measurements has been observed using the heavy-water-based correlation. Figure 8 compares measured dryout powers against predicted dryout powers.

Other than low dryout power measurements for the bundle with a uniform axial power profile, the majority of the dryout power measurements were underpredicted. Overall, the average prediction bias is -5.41% with a standard deviation of 4.05%. The prediction bias is defined as

$$Bias = \frac{Predicted\ Dryout\ Power}{Measured\ Dryout\ Power} - 1 \tag{10}$$

The underprediction appears to be worse for the bundle with the non-uniform axial power profile (with an average prediction bias of -7.3%) than that for the one with the uniform axial power profile (with an average prediction bias of -3.3%). Therefore, applying the light-water-based correlation in predicting the heavy-water dryout power measurements would lead to an overprediction by a similar bias. This is consistent with the previous finding that the heavy-water dryout power is lower than the light-water dryout power in a vertical 36-element bundle at the same system-flow conditions [1]. The 7.3% difference observed in this assessment is slight smaller than the 8-9% estimated in the previous analysis for a non-uniform 36-element bundle.

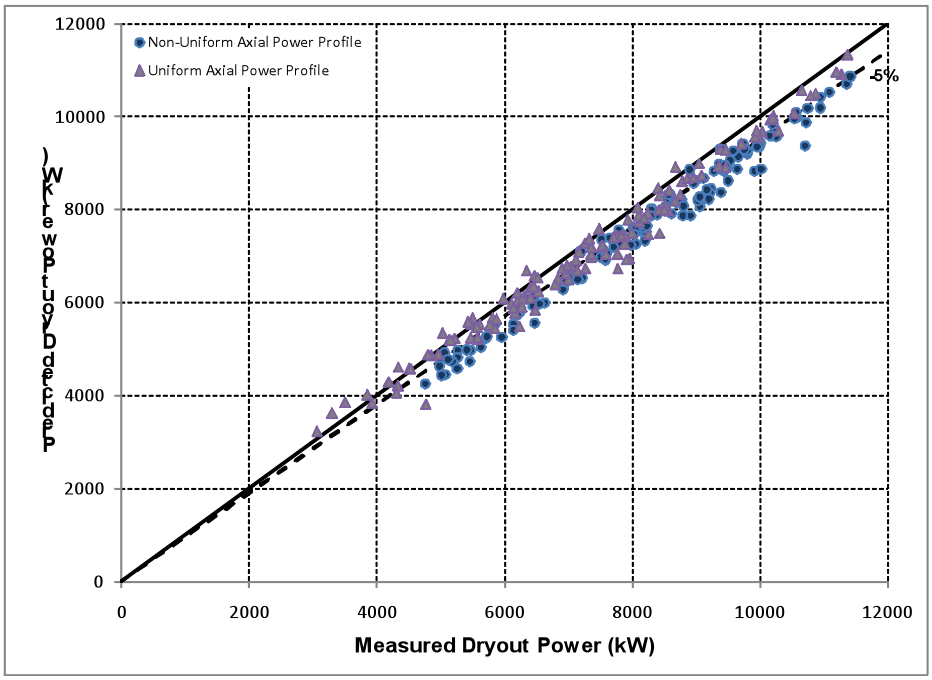

Figure 8 Comparison of Measured Dryout Powers and Predicted Dryout Powers using the Heavy-Water-Based Correlation

7. Conclusion

- Fluid-to-fluid modeling parameters for pressure, mass flux, and CHF in 37-element bundles have been presented.
- High-pressure light-water experiments using 37-element bundle simulators of uniform and non-uniform axial power profile were described.
- A heavy-water-based CHF correlation was derived using transformed heavy-water-equivalent values of CHF and local flow parameters obtained from several light-water experiments. It represents the heavy-water CHF with an average error of 0.5% and a standard deviation of 6.7% for 284 data points.
- An assessment of dryout power predictions has been performed using the heavy-water-based CHF correlation against the light-water dryout power measurements. A systematic underprediction of dryout power measurements has been observed with an average prediction bias of -5.41% and a standard deviation of 4.05%.
- Applying the light-water-based CHF correlation would lead to overprediction of the heavy-water dryout power by about 5% (similar to the observed bias from the reversed analysis illustrated in this study). The assessment result is consistent with that of a previous analysis for the 36-element bundle. However, the magnitude of the difference in dryout power between heavy-water flow and light-water flow is slightly smaller in this assessment (7.3%) than the previous analysis (8-9%).
- Based on the assessment result, applying the light-water-based CHF correlation for heavy-water applications is not recommended. Appropriate heavy-water CHF correlations should be implemented into reactor safety codes for heavy-water applications.

8. References

[1] Becker, K.M., "Measurements of Burnout Conditions for Flow of Heavy Water in Round Tubes", Royal Institute of Technology Report, AE-RTL-1073, 1969.

[2] Barnett, P.G., "An Experimental Investigation to Determine the Scaling Laws of Forced Convection Boiling Heat Transfer. Part 1: the Preliminary Examination Using Burnout Data for Water and Arcton 12", AEEW-R363, 1964.

[3] Ahmad, S.Y., "Fluid-to-Fluid Modelling of Critical Heat Flux: a Compensated Distortion Model", Int. J. Heat Mass Transfer, Vo. 16, pp. 641-662, 1973.

[4] Katto, Y. and Ohno, H., "An Improved Version of the Generalized Correlation of Critical Heat Flux for the Forced Convective Boiling in Uniformly Heated Vertical Tubes", Int. J. Heat Mass Transfer, Vol. 27, pp. 1641-1648, 1983.

[5] Groeneveld, D.C., Kiameh, B.P. and Cheng, S.C., "Prediction of Critical Heat Flux (CHF) for Non-aqueous Fluids in Forced Convective Boiling", Proc. of the 8th Int. Heat Transfer Conference, San Francisco, U.S.A., August, Vol. 5, pp. 2209-2214, 1986.

[6] Tain, R., "An Investigation of CHF Fluid-to Fluid Scaling and Multi-Fluid Prediction Techniques", Ph.D. Thesis, University of Ottawa, 1994.

[7] Leung, L.K.H. and Groeneveld, D.C., "Fluid-to-Fluid Modelling of Critical Heat Flux in 37-Element Bundles", Proc. 21st Nuclear Simulation Symposium, Ottawa, Ontario, Sept. 24-26, 2000.

[8] Leung, L.K.H., "Assessment of Boiling-Length-Average Heat-Flux Approach for Predicting Dryout Power in CANDU 37-Element Bundles", Proc. 13th International Topical Meeting on Nuclear Reactor Thermal Hydraulics (NURETH-13), Kanazawa City, Ishikawa Prefecture, Japan, September 27-October 2, 2009, Paper No. 1384.

[9] Ahmad, S.Y., Nickerson, J.R. and Midvidy, W.I., "Critical Heat Flux Experiments in a Horizontal 37-element Bundle Cooled by Water and Freon", Proc. of the 7th Int. Heat Transfer Conference, Munich, Germany, September, 1982.